ISSN 1063-7834, Physics of the Solid State, 2013, Vol. 55, No. 3, pp. 466–475. © Pleiades Publishing, Ltd., 2013.
Original Russian Text © S.I. Vorob'ev, A.L. Getalov, E.I. Golovenchits, E.N. Komarov, V. P. Koptev, S.A. Kotov, I.I. Pavlova, V.A. Sanina, G.V. Shcherbakov, 2013, published in Fizika Tverdogo Tela, 2013, Vol. 55, No. 3, pp. 422–430.

MAGNETISM

Investigation of the $GdMn_2O_5$ Multiferroic by the μSR Method

S. I. Vorob'ev[a], A. L. Getalov[a], E. I. Golovenchits[b], E. N. Komarov[a], V. P. Koptev[a, †], S. A. Kotov[a], I. I. Pavlova[a], V. A. Sanina[b], and G. V. Shcherbakov[a]

[a] *Konstantinov Petersburg Nuclear Physics Institute, National Research Centre "Kurchatov Institute," Orlova Roshcha, Gatchina, Leningrad oblast, 188300 Russia*

e-mail: vsiloa@pnpi.spb.ru

[b] *Ioffe Physical-Technical Institute, Russian Academy of Sciences, Politekhnicheskaya ul. 26, St. Petersburg, 194021 Russia*

Received July 2, 2012

Abstract—The $GdMn_2O_5$ multiferroic (a ceramic sample and a sample consisting of a large array of randomly oriented single crystals with linear dimensions 2–3 mm) has been studied by the μSR method within the temperature range 10–300 K. Three anomalies in the temperature behavior of the parameters of the muon polarization relaxation function, namely, close to the phase transition driven by the onset of long-range magnetic order in the manganese ion subsystem ($T_{N1} = 40$–41 K), near the lock-in transition initiated by an abrupt change of the wave vector of magnetic order ($T_L = 35$ K), and close to the Gd^{3+} ion ordering temperature ($T_{N2} = 15$ K), have been found. An analysis of the time spectra of muon spin precession in the internal magnetic field of the samples has revealed two positions of preferable muon localization sites in samples, which differ in precession frequencies and the character of their behavior with temperature. The lower-frequency precession driven by Mn^{4+} ions, ferromagnetic Mn^{4+}–Mn^{4+} + muonium complexes, and Gd^{3+}ions is observed throughout the temperature region $T < T_{N1}$ and is practically independent of temperature. At temperatures $T < T_L = 35$ K, a higher-frequency precession associated with Mn^{3+} ions appears also. It is characterized by a temperature dependence $\sim(1 - T/T_{N1})^{\beta}$ with the index $\beta = 0.39$, which is typical of Heisenberg-type 3D magnets. For $T < T_{N1}$, a deficiency of the rest total asymmetry is observed. This phenomenon can probably be assigned to formation of muonium, which suggests that charge transfer processes play an important role in formation of long-range magnetic order.

DOI: 10.1134/S1063783413030311

1. INTRODUCTION

The development of materials with controllable magnetic and electrical properties gives new impetus to studying multiferroics with close temperatures of magnetic and ferroelectric orderings, which are characterized by strong magnetoelectric interaction. Specific examples of multiferroics of this type are $RMnO_3$ rare-earth manganites with perovskite structure [1, 2] and the RMn_2O_5 family of crystals (R stands here for the rare-earth ion, as well as Y and Bi) [3–5].

At room temperature, RMn_2O_5 crystals possess orthorhombic symmetry with space group *Pbam*. They have a complex crystal structure containing Mn^{3+} and Mn^{4+} ions in different lattice sites, which differ in the type of oxygen environment ($Mn^{4+}O_6$ octahedra and $Mn^{3+}O_3$ pyramids) [5]. The competing Mn–Mn and Mn–R magnetic interactions initiate formation of complex magnetic structures in these crystals. The ferroelectric ordering in RMn_2O_5 is most probably driven by special types of charge and magnetic orderings, which break the central symmetry of the lattice [6, 7]. The charge and spin orderings in a chain of manganese ions along the b axis are described by alteration of manganese ions of different valences, which differ also in mutual spin orientation ($Mn^{3+}_{\uparrow}$–$Mn^{4+}_{\uparrow}$–$Mn^{3+}_{\downarrow}$ chains). In the undistorted *Pbam* structure, the distances $d_{\uparrow\uparrow}$ (between $Mn^{3+}_{\uparrow}$ and $Mn^{4+}_{\uparrow}$ ions with parallel spin orientation) and $d_{\uparrow\downarrow}$ (between $Mn^{3+}_{\downarrow}$ and $Mn^{4+}_{\uparrow}$ ions with antiparallel spin orientation) are the same. The exchange interactions between Mn^{3+}–Mn^{4+} pairs with different spin orientations differ. This results in a shortening of the $d_{\uparrow\uparrow}$ distances as compared with $d_{\uparrow\downarrow}$, a factor accounting for the symmetry lowering down to the noncentral $Pb2_1m$ one and formation of the ferroelectric state [6, 7].

Cooling initiates in RMn_2O_5 crystals a successive series of phase transitions [3–5]. Long-range magnetic order with an incommensurate phase sets in at the Néel temperature $T_{N1} \approx 40$–45 K. It is specified by a wave vector $\mathbf{q}(1/2, 0, z)$, where $z = 0.25$–0.37,

† Deceased.

depending on the type of the R^{3+} ion [5]. Close to $T_L \approx$ 35 K, a lock-in transition occurs to change in a jump the wave vector of the magnetic structure, which at $T < T_L$ becomes commensurate with a wave vector $\mathbf{q}(1/2, 0, 1/4)$. Close to this temperature, at $T_{C1} \approx T_L$ ferroelectric ordering with the polarization oriented along the *b* axis of the crystal sets also in RMn_2O_5. As the temperature is lowered still more, one sees another phase transition to occur close to $T_{C2} \approx 20$–25 K, which is accompanied by a steep variation of the electric polarization. Here, the commensurate magnetic phase converts to another, an incommensurate phase. Finally, at temperatures $T_{N2} \leq 10$ K long-range magnetic order sets in the system of R^{3+} magnetic ions. This succession of phase transitions was identified in studies of some RMn_2O_5 crystals by neutron diffraction [4, 5].

In this study, we have addressed the problem of investigation of specific features in the $GdMn_2O_5$ magnetic structure by the μSR method. The large cross section of neutron absorption by Gd nuclei argues against the possibility of studying the magnetic structure of this crystal by neutron diffraction. At the same time, addressing this goal with μSR is possible and, as illustrated by the specific example of our preceding study by this method of the $EuMn_2O_5$ manganite [8], this approach offers a possibility of gaining information on some details of the magnetic structure and specific features of phase transitions impossible to obtain by integrated methods of investigation.

There is presently a fairly rich experimental information concerning the magnetic and ferroelectric properties of $GdMn_2O_5$ obtained by integral approaches. One has studied electric polarization and magneto-electric (ME) effect [9–12], magnetization, and the effect of a strong magnetic field on magnetostriction, polarization, and magnetic susceptibility [12, 13], dielectric permittivity and magnetic susceptibility, microwave and ME dynamics [13, 14]. In these cases, the succession of phase transitions revealed in $GdMn_2O_5$ is, on the whole, similar to the series of phase transitions observed in studies of other RMn_2O_5 crystals by neutron diffraction. Some differences, however, have been revealed to exist too.

The magnetic state of $GdMn_2O_5$ is mediated by the subsystems of the Mn^{3+}, Mn^{4+}, and Gd^{3+} ions. As in other RMn_2O_5 crystals, long-range magnetic order sets in $GdMn_2O_5$ at the Néel temperature $T_{N1} \approx 40$ K. For $T < T_{N1}$, $GdMn_2O_5$ demonstrates the following sequence of phase transitions. The transition near $T_L = 35$ K may be considered to be similar to the lock-in transition in other RMn_2O_5 compounds occurring into the commensurate structure with wave vector $\mathbf{q}(1/2, 0, 1/4)$. But, contrary to expectations, one does not observe in $GdMn_2O_5$ close to this temperature the transition to the ferroelectric state. This transition realizes at a lower temperature $T_{C1} \approx 30$ K (literature demonstrates a scatter in the values of $T_{C1} = 25$–30 K). At $T_{C2} = 20$–22 K, there is a phase transition accompanied by a sharp change of electric polarization. Finally, at $T_{N2} = 15$ K a phase transition establishing a long-range magnetic order in the Gd^{3+} ion system obtains.

Because the Gd^{3+} ion features the highest magnetic (pure spin) moment ($7/2\ \mu_B$) among all the R^{3+} ions, one could expect the Gd^{3+} ions to exert a strong influence on the properties of the $GdMn_2O_5$ compound. Indeed, one has observed an effect of Gd–Mn exchange interaction in the Gd–Mn system on the ME dynamics and phase transitions in strong magnetic fields [12–14]. The shift of the ferroelectric phase transition point in $GdMn_2O_5$ to lower temperatures compared with other RMn_2O_5 crystals could be assigned to the effect of this exchange interaction [14]. What is more, long-range magnetic order in the Gd^{3+} ion subsystem emerges at a temperature higher than that in other RMn_2O_5 compounds.

The μSR study of $GdMn_2O_5$ conducted in the present work has demonstrated the significant role played by charge transfer processes between Mn^{3+}–Mn^{4+} pairs of ions in formation of long-range magnetic order. A similar effect was revealed in a μSR study of $EuMn_2O_5$ [8], which strongly suggests that the effect of charge transfer between manganese ions of different valences in RMn_2O_5 multiferroics follows a common pattern. Studies of the second optical harmonic in $TbMn_2O_5$ [15] likewise stressed the important role associated with charge transfer processes.

2. EXPERIMENTAL DETAILS AND TREATMENT OF EXPERIMENTAL DATA

The experiments were carried out at μSR-setup positioned at the exit from the muon beam of the Petersburg Nuclear Physics Institute synchrocyclotron. The muon beam had momentum $p_\mu = 90$ MeV/*c*, momentum spread (FWHM) $\Delta p_\mu / p_\mu = 0.02$, and longitudinal polarization $P_\mu \sim 0.90$–0.95. The samples were fixed in a cryostat whose temperature could be set and controlled in the 10–300-K region to within ~0.1 K. The Helmholtz coil system used permitted one to sustain in the bulk of a sample an external magnetic field of up to 1.5 kOe. The stability of coil power supply was maintained at a level of $\sim 10^{-3}$. The magnetic field homogeneity at the sample was estimated by μSR measurements on a nonmagnetic sample (Cu). The parameter λ of the muon P_μ polarization relaxation rate ($P_\mu \sim \exp(-\lambda t)$) in Cu is $\lambda = (0.0053 \pm 0.0031)\ \mu s^{-1}$, thus making it possible to conduct μSR measurements in magnetic materials.

The time spectra of positrons produced in muon decay were measured in two ranges (10.0 and 1.1 μs)

with scale division values 4.9 and 0.8 ns/channel, respectively.

For μSR studies requiring large-volume samples two $GdMn_2O_5$ samples were fabricated. The first sample was a ceramic disk 30 mm in diameter and 12 mm thick prepared by solid-state reaction synthesis. The grains of its structure were a few tens of microns in size. The structure and single-phase composition of the ceramic sample were attested by X-ray phase analysis. The second sample represented actually an array of $GdMn_2O_5$ single crystals with linear dimensions ~2–3 mm grown by spontaneous crystallization. The single crystals were placed in a container of the same size as the one for the ceramic sample. The μSR measurements were conducted on single crystals of the same lot on which measurements of the magnetic and dielectric susceptibilities and magnetic dynamics were performed [13, 14]. Both samples (referred to in what follows as the ceramic sample and the single-crystal-combined sample) had random orientation of crystal axes and differed only in the sizes of their "structural units."

A detailed description of the equipment employed, data recording system and method of data treatment can be found in our previous publications [16, 17].

The experimental time spectra of muon decay positrons were described by the following relation

$$N_e(t) = N_0\exp(-t/\tau_\mu)[1 + a_sG_s(t) + a_bG_b(t)] + B, \quad (1)$$

where N_0 is the normalization constant, a_s and a_b are asymmetries of the muon decay positrons which stopped in the sample (a_s) and in parts of the equipment (a_b); $G_s(t)$ and $G_b(t)$ are the corresponding muon polarization relaxation functions, and B is the random coincidence background. The level and the time structure of the latter were derived from an analysis of the events that occurred in the initial region of the time spectrum (before the muon stopped in the sample), where neither the relevant nor background events produced in the body of the equipment could occur. The asymmetry a_b and the parameters of the background function $G_b(t)$ for each sample were obtained from an analysis of the time spectrum which was measured in an external magnetic field at the Néel temperature of the sample ($T < T_{N1}$). In this case, the observed amplitude of precession frequency in a specified external magnetic field is equal to the contribution a_b to total asymmetry. In the same treatment one finds the polarization relaxation rate λ_b of the muons that had stopped in the body of the equipment. Thus we come to complete determination of the temperature-independent term $a_bG_b(t) = a_b\exp(-\lambda_bt)$.

The processing of experimental data was based on the standard assumption of factorization of the relaxation function

$$a_sG_s(t) = a_sG_d(t)G_{st}(t). \quad (2)$$

Here, $G_d(t) = \exp(-\lambda t)$ is the dynamic relaxation function describing the magnetic fluctuations of magnetic field in a sample with time during the muon lifetime. $G_{st}(t)$ is the static relaxation function whose actual form and parameters are governed by the distribution of local magnetic fields in the areas preferable for muon localization after its slowing down in the sample and completion of the process of its thermalization. In the vicinity of these positions of muon localization, fast short-term fluctuations set in, and the $G_{st}(t)$ function varies much faster than $G_d(t)$ does. In these conditions, the $G_{st}(t)$ relaxation function can be factorized [18–21].

Introduction of the concept of residual asymmetry a_s provides a possibility of taking into account the loss of the initial (total) asymmetry a_0 as a result of emergence of additional muon depolarization channels brought to life by variation of the sample temperature. The parameter a_0 was derived from experimental data obtained in an external magnetic field when the sample resided in paramagnetic state.

3. RESULTS OF THE EXPERIMENT

The experimental data obtained were used to derive the temperature dependences of the parameters specifying the polarization relaxation function of the muons which stopped in the sample.

The behavior with temperature of the dynamic relaxation rate λ in the 10–80-K interval is visualized in Fig. 1. We carried out measurements at $T = 300$ K as well, and it turned out that the value of λ at $T = 300$ K coincides with that measured at 80 K. Most probably, the parameter λ does not change in the temperature region from 80 K to 300 K. Note the unusually high value of λ (~1 μs^{-1}) which does not change throughout the temperature region covered here, and against this background one observes anomalies near the phase transitions. Such a large value of the background λ in $GdMn_2O_5$ and its independence of temperature may tentatively be ascribed to the existence in the samples, within a broad range of temperature, of limited regions of short-range magnetic order. Measurements of the magnetic susceptibility performed in multiferroics of the RMn_2O_5 family suggest that their Curie–Weiss temperature $\theta_{CW} \gg T_{N1}$, and that there is a fairly high frustration ratio $\theta_{CW}/T_{N1} \approx 6–7$ [22, 23], which implies that RMn_2O_5 crystals are magnetically frustrated multiferroics. It is known that in such systems above the T_{N1} temperature, within the temperature interval specified by the frustration ratio, a strongly correlated paramagnetic state usually evolves [24]. That the background values of λ at $20\text{ K} < T < T_{N1}$ and in the paramagnetic region coincide suggests that a strongly frustrated state of the crystal is present at $T < T_{N1}$ as well.

Anomalies of the λ parameter are observed at phase transition temperatures near which magnetic properties undergo pronounced changes, as established by measurements performed by other methods (Fig. 1), namely: $T_{N1} = 39–41$ K (onset of long-range magnetic order in the manganese ion subsystem); $T_L = 35$ K (lock-in transition involving a change of the wave vector of magnetic ordering to a state commensurate with the lattice), and $T_{N2} = 15$ K (magnetic ordering in the Gd^{3+} ion subsystem). The structural phase transition near 22–26 K observed in measurements of the ME effect and polarization and the onset of ferroelectric ordering at $T \approx 30$ K established in our measurements manifest themselves not so clearly. This appears only natural, because the μSR method is capable of probing the magnetic structure of a material only.

The measurements on the ceramic sample were conducted in two regimes, namely, with the sample cooled from 100 to 15 K, and, subsequently, under heating from 10 to 32.5 K. In the latter case, the sample was first cooled from room temperature down to 10 K (during ~1 hour). As seen from Fig. 1a, within the temperature interval from 20 to 32 K, the $\lambda(T)$ graph reveals hysteresis.

The effect of external magnetic field was also studied at some temperatures. The design of the equipment permitted one to operate with an external magnetic field oriented perpendicular to the muon beam. This is not really essential, because in both samples the axes of individual crystals are isotropically random oriented. We readily see (Fig. 1) that application of a field $H = 280$ Oe brings about a noticeable decrease of the dynamic relaxation rate λ below T_{N1} while practically not affecting its level in the paramagnetic region.

At temperatures 10–15 K, the λ parameter also falls off, particularly steeply for the ceramic sample, most likely as a result of the onset of long-range magnetic order in the subsystem of Gd^{3+} ions. Incidentally, application of a magnetic field at $T > 20$ K and ordering in the Gd^{3+} ion system (at $H = 0$) at $T \le 15$ K lower the λ parameter to about the same level.

We consider the behavior with temperature of the residual asymmetry a_s (Figs. 2 and 3). In the paramagnetic region ($T > T_{N1}$), the magnitude of a_s is practically temperature independent and remains equal to the total asymmetry a_0. We note that the residual asymmetry at $T = 300$ K has the same value as that at 40 K $< T <$ 80 K. At temperatures $T < T_{N1}$, the asymmetry a_s should be equal to $1/3a_0$. The point is that when a sample resides in paramagnetic state, the decay asymmetry of a fully polarized muon beam is a_0. Below T_{N1}, magnetic ordering orients the magnetic field in each crystal of a sample in a specified manner relative to the crystallographic axes. Because, however, the "structural components" proper of the sample are randomly oriented, the effect of the pattern averaged over the axis directions is the same as if for 1/3 of all

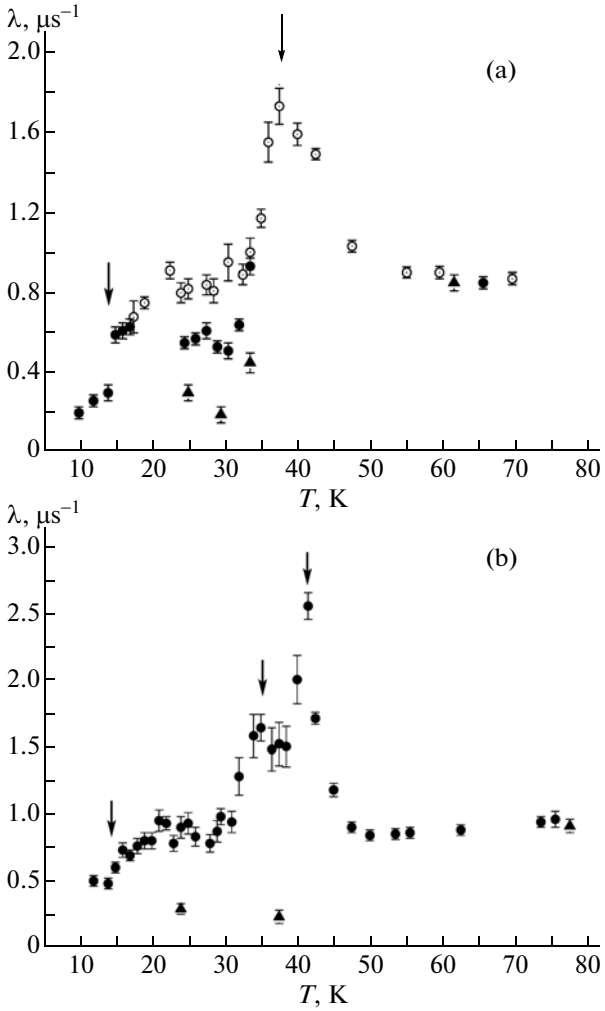

Fig. 1. Temperature dependence of the dynamic relaxation rate λ: (a) ceramic sample and (b) single-crystal sample. Filled dots relate to measurements performed under heating, open dots, to those under cooling, and triangles, to measurements in external magnetic field $H = 280$ Oe. Arrows specify phase transition temperatures.

muons the magnetic field were aligned with their spin (and maintained the decay asymmetry equal to a_0), while for the remaining 2/3 of all muons it were cross-oriented, initiated muon spin precession and, as a consequence, an asymmetry equal to zero. In the final count, the observed asymmetry turns out to be $1/3a_0$. The experimentally observed value of a_s drops, however, substantially lower than $1/3a_0$, particularly for the sample combined of single crystals. This suggests emergence of an additional channel of muon polarization loss for $T \le T_{N1}$. This channel could be the formation of muonium $Mu = \mu^+e^-$. It is probable that below T_{N1} the probability of charge (electron) transfer between the Mn^{3+} and Mn^{4+} ions (double exchange) increases to make possible muonium formation. The

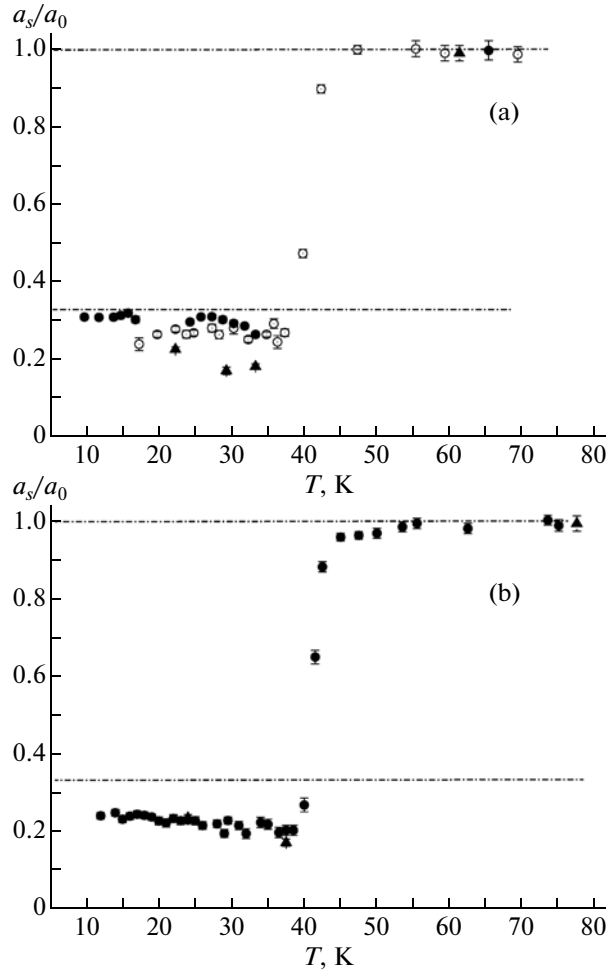

Fig. 2. Temperature dependence of residual asymmetry a_s normalized against total asymmetry a_0: (a) ceramic sample and (b) single-crystal sample. The levels of normalized asymmetry $a_s/a_0 = 1/3$ ($T < T_{N1}$) and $a_s/a_0 = 1$ ($T > T_{N1}$) are identified by dot-and-dash lines. Filled dots refer to measurements performed under heating, open ones, to those under cooling, and triangles, to measurements in external magnetic field $H = 280$ Oe.

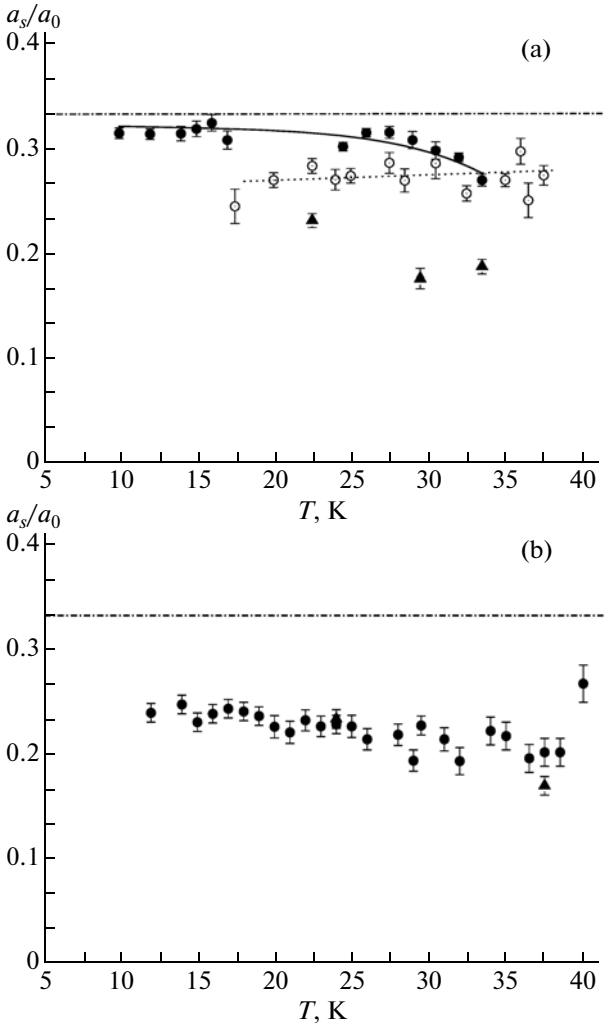

Fig. 3. Same as in Fig. 2 but for the temperature region $T < T_{N1}$.

effect of muon polarization loss was observed earlier in studies of $EuMn_2O_5$ manganite samples [8].

Application of an external magnetic field brings about an increase of asymmetry loss for the ceramic sample only, while not affecting in any way the asymmetry a_s for the sample of single crystals (Figs. 2 and 3).

Two modes chosen for variation of the temperature of the ceramic sample produce two branches illustrating the behavior of residual asymmetry with hysteresis (Fig. 3a). The sample combined of single crystals was studied under heating only. Incidentally, hysteresis was revealed earlier in a study of the dielectric permittivity, magnetic susceptibility and magnetic dynamics of $GdMn_2O_5$ at $T \le T_{N1}$ [13, 14].

The fast processes involved in muon depolarization can be specified with the static relaxation function of a collinear ferromagnet

$$a_s G_{st}(t) = \sum_i G^i_{st}(t), \qquad (3)$$

$$G^i_{st} = a_i[1/2 + 2/3\cos(\Omega_i t)\exp(-\Delta_i t)], \quad i = 1, 2.$$

Here, a_i are partial amplitudes of the observed muon spin precession frequencies in a local internal magnetic field ($a_1 + a_2 = a_s$). The frequencies $\Omega_i = 2\pi F_i(T)$ and the precession damping rates $\Delta_i(T)$ depend on the magnitude of the local magnetic field and the scatter of these fields in the vicinity of the points of localization of a muon at the instant of its stopping in the sample.

Figure 4 exemplifies graphically the relaxation functions $G_s(t)$ for two values of the temperature of the ceramic sample, which were derived from the experi-

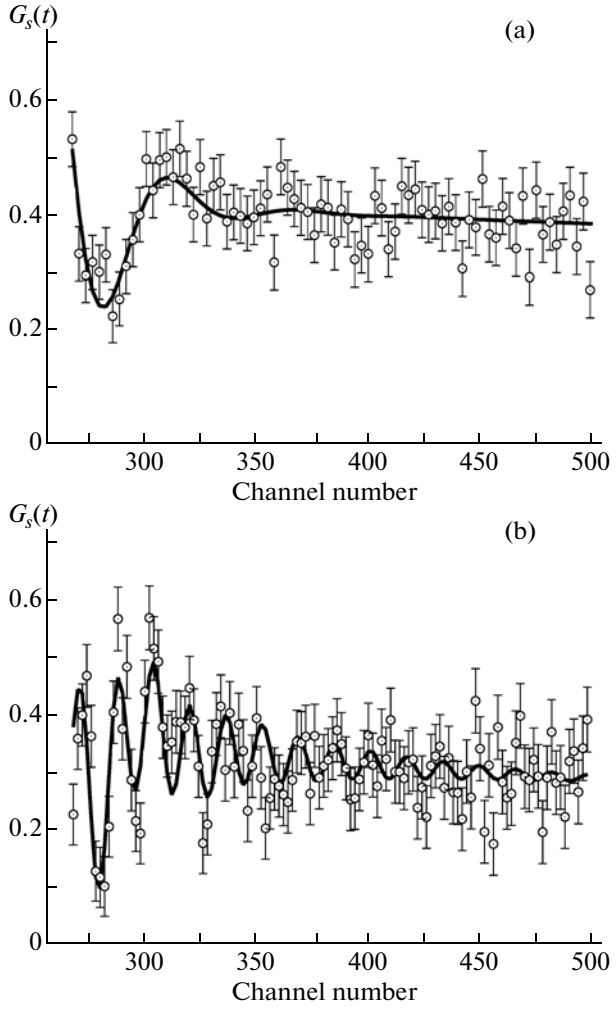

Fig. 4. Relaxation function $G_s(t)$ at temperatures (a) T_L = 35 K and (b) T_{C2} = 22 K for the ceramic sample. Solid lines were obtained by least-squares fitting of the parameters with (a) one or (b) two precession frequencies; the value of 1 channel is 0.8 ns.

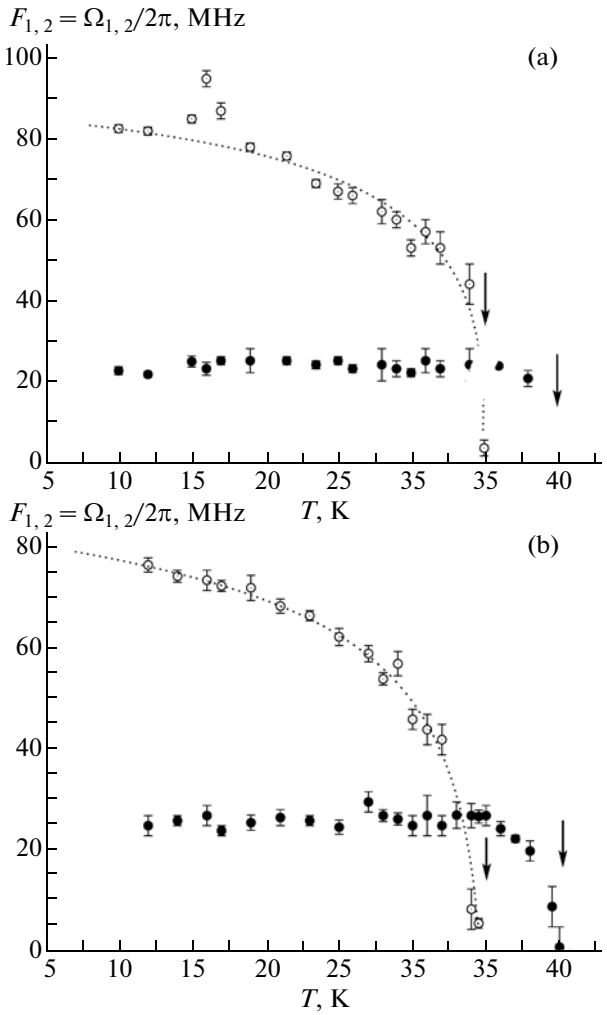

Fig. 5. Temperature dependences of precession frequencies in the internal magnetic field of the sample: (a) ceramic sample and (b) single-crystal sample. Filled dots relate to frequency F_1, and open ones, to frequency F_2. Arrows identify phase transition temperatures T_L = 35 K and T_{N1} = 40 K. Dotted curve was obtained by least-squares fitting: $F_2 \sim (1 - T/T_L)^{\beta}$, T_L = 35 K; $\beta = 0.39 \pm 0.02$.

mental data. At T_L = 35 K, a state with only one preferable site of localization of a muon with one precession frequency is realized in the sample (Fig. 4a). At the temperature T_{C2} = 22 K, two such localization points with two precession frequencies exist (Fig. 4b).

The behavior with temperature of the observed muon precession frequencies in the internal magnetic field is visualized in Fig. 5. One immediately sees a number of features in these graphs. Just below T_{N1} one observes within the temperature interval from 40 to 35 K only one frequency F_1, which reaches fairly steeply a plateau in the temperature dependence (at a level of 20–25 MHz). At a temperature T_L = 35 K, an additional precession appears in both samples at a frequency F_2, which grows monotonically with decreasing temperature. The temperature dependence of frequency F_2 can be approximated in regions outside the phase transition zones with the Curie–Weiss function $F_2 \sim (1 - T/T_L)^{\beta}$ with the index $\beta = 0.39$ characteristic of Heisenberg-type 3D magnets.

The partial contributions a_1 and a_2 for each precession frequency to the residual asymmetry a_s were determined with an error larger than those of the precession frequencies (Fig. 6). Nevertheless, some features can be established with an acceptable degree of reliability; as an example, the partial asymmetry a_1 corresponding to the precession frequency F_1 falls down at $T_L \approx 35$ K, but remains within the temperature interval 20–35 K less than the partial asymmetry a_2 corresponding to the precession frequency F_2. At lower temperatures, the behavior of the partial asym-

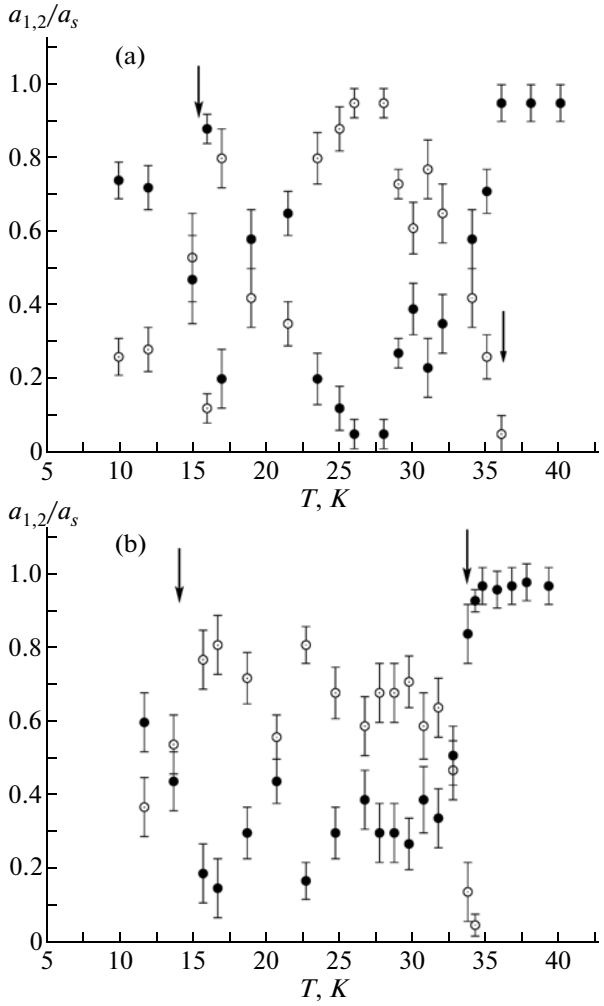

Fig. 6. Temperature dependences of normalized partial contributions: (a) ceramic sample and (b) single-crystal sample. Filled dots relate to the parameter a_1/a_s, and open ones, to a_2/a_s. Arrows identify phase transition temperatures $T_{N2} = 15$ K and $T_L = 35$ K.

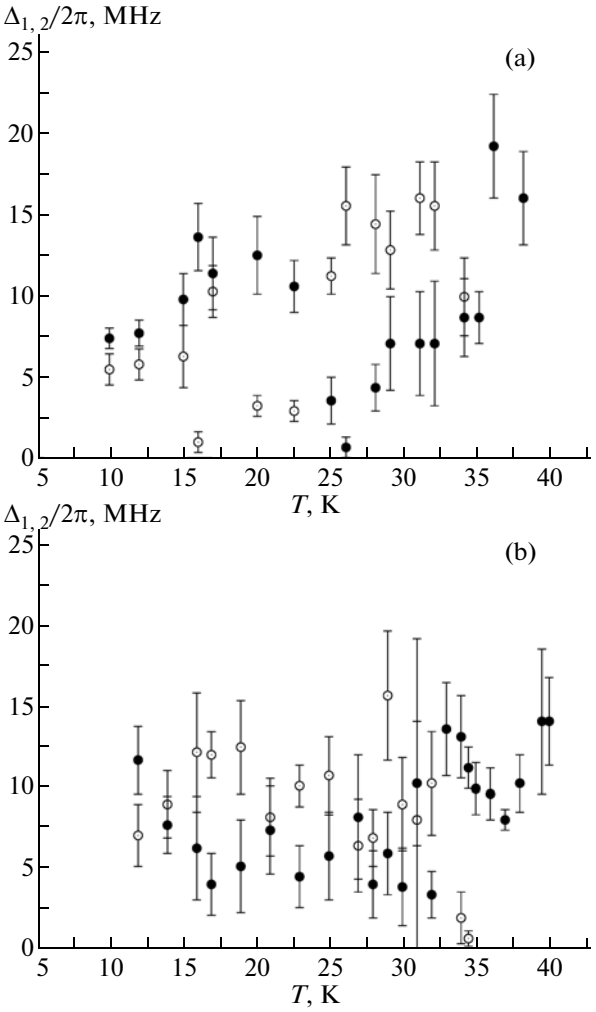

Fig. 7. Temperature dependences of static relaxation rates: (a) ceramic sample and (b) single-crystal sample. Filled dots relate to the parameter $\Delta_1/2\pi$, and open ones, to $\Delta_2/2\pi$.

metries is determined with a large error, particularly for the sample fabricated from single crystals. The temperature dependences of the static relaxation rates $\Delta_{1,2}$ are determined with a still larger error (Fig. 7), which makes their adequate analysis practically impossible. This likewise argues for the crystal being strongly frustrated at $T < T_{N1}$ as well.

4. DISCUSSION OF THE RESULTS

The evolution with temperature of the parameters of the muon relaxation function observed in this study is driven primarily by changes of the magnetic state and phase transitions in the crystals under investigation.

A specific feature of the $R\mathrm{Mn_2O_5}$ manganites consists in a layer-by-layer arrangement of magnetic ions in the lattice; indeed, Mn^{3+} ions occupy the layer $z = 1/2c$, Mn^{4+} ions—layers $z = 1/4c$ and $z = 3/4c$, and ions R^{3+}, the layer $z = 0$ [5]. Long-range magnetic order is sustained by exchange interactions between pairs of Mn ions both in the same and different valence states. A positively charged muon is naturally localized near an electrically negative oxygen ion in the Mn–O–Mn chain. The spin precession frequency of a muon in a local magnetic field and the probability of its localization near different Mn ion pairs is determined by the magnitudes of exchange interaction among these ions.

There are three different chains of indirect exchange interaction involving oxygen ions: Mn^{3+}–O(1)–Mn^{3+}, Mn^{4+}–O(4)–Mn^{4+} and Mn^{3+}–O(3)–Mn^{4+} (Fig. 8). Besides, there exists a substantially stronger double exchange [25, 26] realized through e_g

electron transfer between Mn^{3+} and Mn^{4+} ions ($Mn^{3+} \leftrightarrow Mn^{4+} + e_g$). The Mn^{3+} ion has one delocalized e_g electron bound strongly to the oxygen ion, and three localized t_{2g} electrons. The Mn^{4+} ion has only three localized t_{2g} electrons, which are bound weaker to the oxygen ion. As a result, exchange interaction in the Mn^{3+}–O(1)–Mn^{3+} chain is substantially stronger than that in the Mn^{4+}–O(4)–Mn^{4+} chain. This accounts for our assumption that the higher precession frequency F_2 and the probability to find a muon close to the O(1) ion observed below the transition temperature $T_{N1} = 40$ K define the situation in which the muon is localized in the Mn^{3+}–O(1)–Mn^{3+} chains.

A specific situation is realized with Mn^{3+}–Mn^{4+} pairs between which double exchange is possible. This exchange is described by a Hamiltonian [25, 26]

$$H_{DE} = -t\cos(\theta/2). \quad (4)$$

Here, θ is the angle between the directions of spins S_1 and S_2 of neighboring Mn^{3+} and Mn^{4+} ions, and t is the charge transfer integral ($t \approx 300$ meV). This exchange mechanism gives rise to ferromagnetic orientation of the S_1 and S_2 spins and of the spin of the e_g electron in the original antiferromagnetic RMn_2O_5 matrix [25, 26]. In view of the possibility for a muon to stop close to such a ferromagnetic Mn^{3+}–Mn^{4+} pair, one can visualize a scenario of muonium formation (when a muon absorbs the e_g electron involved in the double exchange). This results in formation of a ferromagnetic complex Mn^{4+}–Mn^{4+} + muonium. Near this complex, frustration sets in the original magnetic and charge order, which damps efficiently the internal field at temperatures below 40 K. Besides, this increases efficiently the number of Mn^{4+} ions in whose vicinity muon localization results in a lower precession frequency and a decrease of the corresponding partial amplitude a_1 (Fig. 6). We note also that the behavior of the ferromagnetic moments of Mn^{4+} ion pairs (belonging to muon complexes) does not depend on temperature. For this reason, the lower precession frequency F_1 is practically temperature independent (Fig. 5).

Significantly, transformation of Mn^{3+}–Mn^{4+} ion pairs into the muonium complex Mn^{4+}–Mn^{4+} + muonium may account for the decrease of residual asymmetry a_s below 40 K (Figs. 2, 3). This mechanism is apparently typical of all RMn_2O_5 crystals containing both Mn^{3+} and Mn^{4+} ions. This effect was observed by us earlier in $EuMn_2O_5$ [8]. Theoretical investigation [6, 7] revealed that the charge ordering processes and transfer among Mn ions in different valence states (double exchange) play an important role in formation of the multiferroic state in RMn_2O_5 [5].

As already pointed out, $GdMn_2O_5$ crystals are strongly frustrated systems within a broad temperature range. Studies of microwave radiation absorption, dielectric permittivity and magnetic susceptibility revealed below T_{N1} hysteresis phenomena [14, 15]. Formation of the Mn^{4+}–Mn^{4+} + muonium complexes increases the degree of crystal frustration because of the additional spin and charge distortions and entails intensification of hysteresis phenomena.

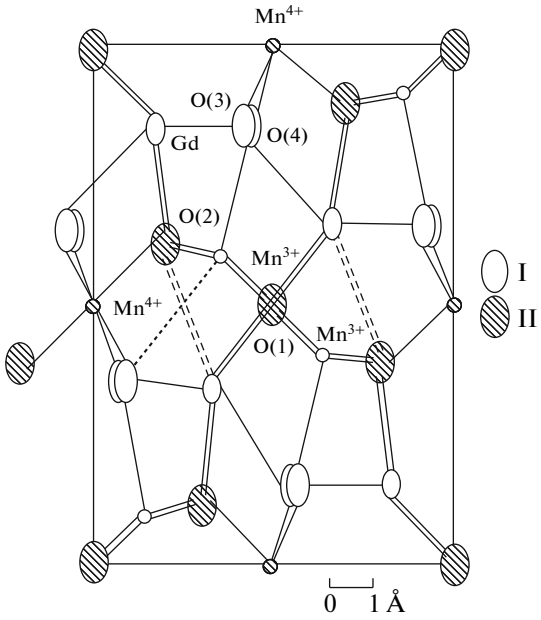

Fig. 8. Crystal structure of $GdMn_2O_5$: (I) ions in planes $z = 0$ and $z = 1/2c$, and (II) ions in planes $z = 1/4c$ and $z = 3/4c$. Solid lines are the bonds between nearest ions, and dotted line is the distant bond for Mn^{3+} ion.

Let us address now the differences in the extent of a_s asymmetry losses in the ceramic and single crystal-arranged samples, as well as the different effect of magnetic field on a_s in these samples. Asymmetry losses in a single crystal-arranged sample are larger than those in a ceramic one. At the same time, application of a magnetic field increases the magnitude of a_s in the ceramic sample up to approximately the level of losses in the sample combined of single crystals (Figs. 2 and 3). The sizes of grains in the ceramic sample are smaller by far than that of separate single crystal sizes in the corresponding sample. Also, the boundaries between ceramic grains are considerably thinner than gaps between separate single crystals. Charge transfer among individual single crystals is impossible, whereas it can cross (although not freely) the boundaries separating grains in a ceramic. As a result, in the ceramic sample the whole bulk of the crystal (both the grains themselves and the boundaries) take active part in the process of charge transfer among Mn ions in different valence states, whereas in the sample combined of single crystals this occurs in the bulk of individual single crystals only. The developed surface of boundaries among grains in the ceramic sample reduces the

probability of charge transfer processes across these boundaries. The increase of asymmetry losses initiated in the ceramic sample by application of an external magnetic field suggests that it is pinning of the random spin orientation of Mn^{3+} and Mn^{4+} ion pairs at these boundaries that acts as the main factor blocking charge transfer across the boundaries of ceramic grains. Enhanced spin orientation of the Mn^{3+}–Mn^{4+} ions pairs along the applied magnetic field increases the probability of double exchange, charge transfer among these pairs (see Eq. (4)) and formation of muonium complexes. This entails the increase of asymmetry losses in the ceramic sample.

In the vicinity of $T = 22$–25 K, the contributions of the a_1 and a_2 partial amplitudes to the total asymmetry a_s change, with the a_1 contribution decreasing noticeably. These changes are more clearly pronounced for the ceramic sample, although the associated accuracy of determination of the partial amplitudes drops in both samples (Fig. 6). As already mentioned, integral methods reveal at these temperatures a structural phase transition involving a sharp change of electric polarization. Near $T = 25$–30 K, ferroelectric ordering develops in $GdMn_2O_5$, in which, by analogy with other RMn_2O_5 crystals, symmetry drops to the noncentral $Pb2_1m$ [6, 7]. The transition to the ferroelectric state at 30 K was studied on $ErMn_2O_5$ [27] by x-ray diffraction in synchrotron radiation. It was established that this transition involves displacement of oxygen ions in the Mn–O–Mn chains, which entails a change of interionic separations and bond angles in the Mn–O–Mn chains. This should bring about redistribution of partial asymmetries.

Below 22 K, the magnetic subsystem of Gd^{3+} ions also comes to life. The response of Gd^{3+} ions becomes dynamic close to the temperature $T_{N2} = 15$ K. Magnetic ordering develops in the Gd^{3+} ion system. One could have expected this to initiate formation of a third precession frequency. This does not happen, however, and one observes instead only redistribution of the partial asymmetry amplitudes indicating relative growth of the effective Mn^{4+} ion concentration. One could mention in this connection that the magnetic states of Gd^{3+} ions (which reside in the S state) and of Mn^{4+} ions (with three localized electrons in t_{2g} state and frozen orbital moments in ground state) are similar, and, possibly, the internal magnetic field in the vicinity of Gd^{3+} ions is similar to that near the Mn^{4+}–Mn^{4+} + muonium complexes.

5. CONCLUSIONS

The $GdMn_2O_5$ samples (a ceramic one and a sample composed of single crystals) have been studied by the μSR method.

Anomalies have been revealed in the temperature dependence of the parameters of the muon polarization relaxation function close to three phase transitions, to wit, $T_{N1} = 40$ K, $T_L = 35$ K, and $T_{N2} = 15$ K.

It has been established that below the temperature of the onset of long-range magnetic order, $T_{N1} = 40$ K, the Mn ion system undergoes loss of the total residual asymmetry, which may be assigned to muonium formation and is indicative of the significant role played by the processes of charge transfer among Mn^{3+} – Mn^{4+} ion pairs in the formation of long-range magnetic order in the $GdMn_2O_5$ multiferroic.

Two frequencies of muon precession in the internal field of samples have been identified. They differ significantly in the behavior with temperature. The lower frequency F_1 appears in the region $T_{N1} < 40$ K and is practically temperature-independent (except for the immediate vicinity of $T \approx T_{N1}$). The muon spin precession at this frequency owes its existence to Mn^{4+}–O–Mn^{4+} ion chains, formation of single isolated ferromagnetic muonium complexes and an ordered Gd^{3+} ion subsystem. The second, higher precession frequency F_2 appears at temperatures $T < T_L = 35$ K and originates from muon localization close to Mn^{3+}–O–Mn^{3+} ion chains. Its temperature dependence is fitted by the Curie–Weiss law $F_2 \sim (1 - T/T_L)^{\beta}$, with the index $\beta = 0.39$ typical of Heisenberg-type 3D magnets.

The specific features observed in the temperature behavior of the dynamic relaxation rate λ and of the partial contributions a_1 and a_2 to the total residual asymmetry in the vicinity of $T = T_{N2} = 15$ K derive from magnetic ordering in the Gd^{3+} ion system.

The μSR studies show $GdMn_2O_5$ to reside in a strongly frustrated magnetic state within a broad temperature range, both below and above the temperature T_{N1}.

REFERENCES

1. T. Kimura, T. Goto, H. Shintani, K. Ishizaka, T. Arima, and Y. Tokura, Nature (London) **426**, 55 (2003).
2. S.-W. Cheong and M. Mostovoy, Nat. Matter **6**, 13 (2007).
3. N. Hur, S. Park, P. A. Sharma, J. S. Ahn, S. Guha, and S.-W. Cheong, Nature (London) **429**, 392 (2004).
4. Y. Noda, H. Kimura, M. Fukunago, S. Kobayashi, I. Kagomiya, and K. Kohn, J. Phys.: Condens. Matter **20**, 434206 (2008).
5. P. G. Radaelli and L. C. Chapon, J. Phys.: Condens. Matter **20**, 434213 (2008).
6. J. Van den Brink and D. I. Khomskii, J. Phys.: Condens. Matter **20**, 434217 (2008).
7. G. Giovanneti and J. Van den Brink, Phys. Rev. Lett. **100**, 227603 (2008).
8. S. I. Vorob'ev, E. I. Golovenchits, V. P. Koptev, E. N. Komarov, S. A. Kotov, V. A. Sanina, and G. V. Shcherbakov, JETP Lett. **91** (10), 512 (2010).

9. A. Inomata and K. Kohn, J. Phys.: Condens. Matter **8**, 2673 (1996).
10. H. Tsujino and K. Kohn, Solid State Commun. **83**, 639 (1992).
11. M. Fukunago and Y. Noda, J. Phys. Soc. Jpn. **79**, 054705 (2010).
12. Yu. F. Popov, A. M. Kadomtseva, G. P. Vorob'ev, S. S. Krotov, K. I. Kamilov, and M. M. Lukina, Phys. Solid State **45** (11), 2155 (2003).
13. E. I. Golovenchits and V. A. Sanina, JETP Lett. **78** (2), 88 (2003).
14. E. Golovenchits and V. Sanina, J. Phys.: Condens. Matter **16**, 4325 (2004).
15. Th. Lottermoser, D. Meier, R. Pisarev, and M. Fiebig, Phys. Rev. B: Condens. Matter **80**, 100101 (R) (2009).
16. S. G. Barsov, S. I. Vorob'ev, V. P. Koptev, S. A. Kotov, S. M. Mikirtych'yan, and G. V. Shcherbakov, Instrum. Exp. Tech. **50** (6), 750 (2007).
17. S. G. Barsov, S. I. Vorob'ev, E. N. Komarov, V. P. Koptev, S. A. Kotov, S. M. Mikirtych'yan, and G. V. Shcherbakov, Preprint No. 2738, PIYaF (Petersburg Institute of Nuclear Physics, Gatchina, Leningrad oblast, 2007).
18. J. A. Dann, A. D. Hillier, J. G. Armitage, and R. Cywinski, in *Proceedings of the 8th International Conference on Muon Spin Rotation, Relaxation and Resonance, Les Diablerets, Switzerland, August 30–3 September, 1999*, p. 38.
19. V. V. Krishnamurthy, K. Nagamine, I. Wanatabe, K. Nishiyama, S. Ohira, M. Ishikawa, D. H. Eom, and T. Ishikawa, in *Proceedings of the 8th International Conference on Muon Spin Rotation, Relaxation and Resonance, Les Diablerets, Switzerland, August 30–3 September, 1999*, p. 47.
20. R. De Reizi and S. Fanesi. Physica B **289–290**, 209 (2000).
21. C. J. Boardman, R. Cywinski, S. H. Kilcoyne, and C. A. Scott, in *Proceedings of the 6th International Conference on Muon Spin Rotation, Relaxation and Resonance. Maui, Hawaii, United States, May 31–June 11, 1993*, p. 525.
22. A. F. Garcia-Flores, E. Granado, H. Martinho, R. R. Urbano, C. Rettori, E. I. Golovenchits, V. A. Sanina, S. B. Oseroff, S. Park, and S.-W. Cheong, Phys. Rev. B: Condens. Matter **73**, 104411 (2006).
23. E. I. Golovenchits, V. A. Sanina, and V. A. Babinskii, JETP **85** (1), 156 (1997).
24. A. P. Ramirez, *Handbook of Magnetic Materials* (Elsevier, New York, 2001), Vol. 13, p. 423.
25. L. P. Gor'kov, Phys.—Usp. **41** (6), 589 (1998).
26. M. Yu. Kagan and K. I. Kugel', Phys.—Usp. **44** (6), 553 (2001).
27. B. Roeslli, P. Fisher, P. J. Brown, M. Janoschek, D. Sheptyakov, S. N. Gvasaliya, B. Ouladdiaf, O. Zaharko, Eu. Golovenchits, and V. Sanina, J. Phys.: Condens. Matter **20**, 485216 (2008).

Translated by G. Skrebtsov